Coaxial Conjugated Polymer/Quantum Rod Assembly into Hybrid Nanowires with Preferred Quantum Rod Orientation

Jun Ho Hwang,[†,§] Seon-Mi Jin,[†,§] Jinwoo Nam,[‡] and Eunji Lee*[,†]

Correspondence to: Eunji Lee (eunjilee@gist.ac.kr)

[†] School of Materials Science and Engineering, Gwangju Institute of Science and Technology (GIST), Gwangju 61005, Republic of Korea

[‡] Graduate School of Analytical Science and Technology, Chungnam National University, Daejeon 34134, Republic of Korea

1. Solution-Biphase Method vs. One-Pot Addition Method

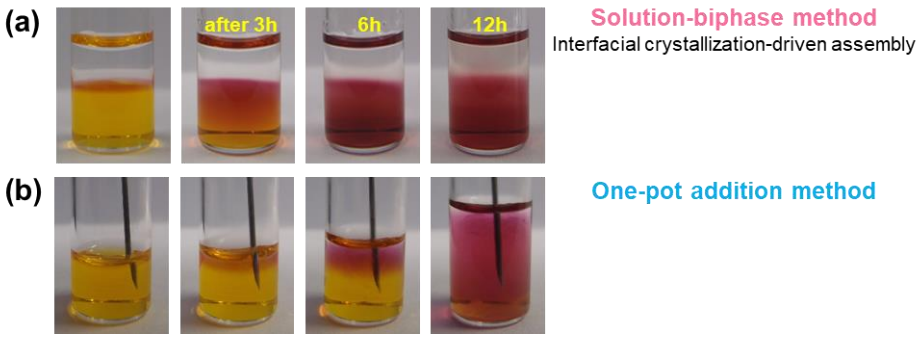

Figure S1. A series of optical photographs representing (a) solution-biphase (top) and (b) one-pot addition methods (bottom) to induce the crystallization-driven assembly of poly(3-hexyl thiophene)-*b*-poly(2-vinylpyridine) (P3HT-*b*-P2VP)/QDs. In the micrographs of (a), the upper layer in the vial is acetonitrile, and bottom layer is P3HT-*b*-P2VP dissolved in chloroform (1 mg/mL of P3HT-*b*-P2VP/QDs, 2:1 (v/v) ratio of chloroform/acetonitrile).

2. Synthesis

Synthesis of P3HT-*b*-P2VP. P3HT-*b*-P2VP was synthesized according to the procedures as reported previously.[S1] Briefly, as a first block, P3HT-based macro chain transfer agent (P3HT macro-CTA) was successfully prepared using a two-step approach involving Suzuki–Miyaura and subsequent DCC coupling reactions. First, P3HT-Br polymer (M_n = 5.8 kg/mol, PDI = 1.18, DP_n = 35) with 92 % regioregularity was produced by varying the ratio of 5-bromo-3,3'-dihexyl-2,2'-bithiopheneto 2-bromo-3-hexylthiophene in polymerization. Then, the palladium-catalyzed Suzuki–Miyaura coupling of P3HT-Br with the tetrahydropyranyl (THP) ether-protected boronic acid (*p*-$THPOC_6H_4B(OH)_2$), followed by aqueous HCl deprotection, provided the desired phenolic P3HT. Subsequently, P3HT macro-CTA was produced via the esterification of the terminal hydroxyl group of P3HT with the carboxyl group of the trithiocarbonate agent in the presence of *N*,*N*'-dicyclohexyl carbodiimide (DCC) and 4-(dimethylamino)pyridine (DMAP). Finally, P3HT-*b*-P2VP was obtained via reversible addition-fragmentation chain transfer (RAFT) polymerization by using P3HT macro-CTA. The resulting products were purified by sequential Soxhlet extractions using methanol, hexane, and chloroform, respectively.

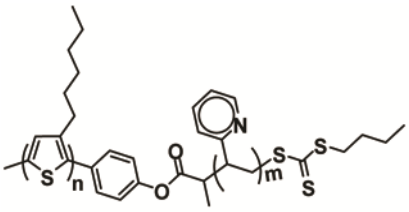

Scheme S1. Chemical structure of P3HT-*b*-P2VP.

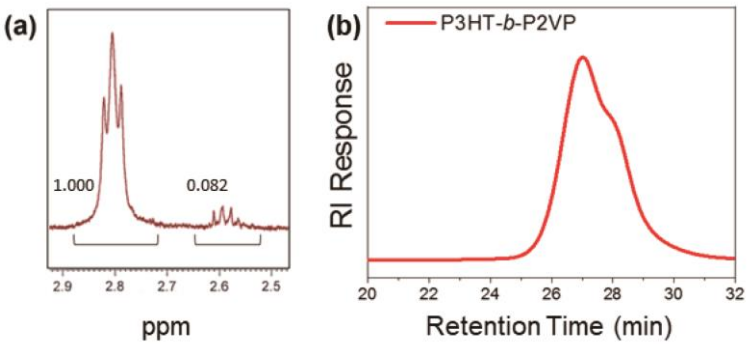

Figure S2. (a) Expanded region from ^{1}H NMR of P3HT block showing the 92% regioregularity. (b) GPC trace of P3HT-*b*-P2VP with THF as eluent.

Table S1. Characteristics of synthesized P3HT-*b*-P2VP used in the study

Polymer	P3HT		P3HT-*b*-P2VP		$M_{n,P2VP}$ (g·mol^{-1})^b	Repeating units P3HT/P2VP	wt% of P2VP^b	Regioregularity^b (%)
	M_n (g·mol^{-1})^a	PDI^a	M_n (g·mol^{-1})^a	PDI^a				
P3HT-*b*-P2VP	5,800	1.18	10,500	1.57	4,600	35/44	45	92

^{a}Determined from GPC in THF calibrated by polystyrene standards. ^{b}Determined from ^{1}H NMR.

Synthesis of TOPO-Capped CdSe QRs.[S2] The CdSe QRs were prepared in "air-free" conditions under argon gas. The cadmium precursor is prepared by a mixture of 25 mg of Cadmium oxide (CdO), 2.0 g of tri-*n*-octylphosphine oxide (TOPO) and 150 mg of *n*-tetradecylphosphonic acid (TDPA) at 80 °C for 2 h. It was done to ensure dissolved oxygen was significant enough to oxidize TOPO in an observable amount. At temperatures above 320 °C, the color of the solution gradually changes from a dark red to a clear colorless, indicating the formation of the Cd precursor. The selenium precursor prepared by dissolving 0.16 M of Se powders in 4 mL of tri-*n*-octylphosphine (TOP) and heating to 60 °C. The Se:TOP solution was optically clear, colorless, and had no visible Se powders. At the 270 °C the 0.16 M Se:TOP was swiftly injected, in the CdO/TOPO/TDPA solution and the solution temperature dropped down to 230 °C. Growth of the CdSe QRs was performed at 260 °C. Growth was allowed to continue for 5 min, then allowed to cool to 50 °C. 5 mL of toluene was injected and the QRs were then precipitated with 10 mL of methanol. Three precipitation and decantation cycles were repeated by dispersing the QRs to toluene and precipitating with methanol. After purification, the CdSe QRs dissolved in chloroform.

Synthesis of TOPO-Capped CdSe/CdS Quantum Tetrapods (QTs).[S3,S4] **1) Synthesis of Zinc Blende (ZB)-CdSe Seeds.** In methanol, Cd nitrate and Na myristate were combined to provide Cd myristate. 0.17 g of Cd myristate was dissolved in 37 mL 1-octadecene and degassed at 90 °C for 1 h in a 50 mL three-neck flask. 0.024 g of Se powder was added to the mixture after cooling to room temperature. The reaction mixture was degassed at 50 °C for 15 min under vacuum and heated to 240 °C under N_2. When the reaction mixture reached 240 °C, 1 mL of oleic acid and 1 mL of oleylamine in 4 mL of 1-octadecene were added. The growth of CdSe can be controlled by measuring the UV-Vis and PL spectra of aliquots taken at various time intervals. Typically, it takes about ~30 min for ~3 nm ZB-CdSe seeds to grow. The reaction mixture was allowed to cool to ambient temperature before being transferred to a N_2-filled glovebox to isolate the seeds. By adding ethanol to the crude solution, ZB-CdSe seeds were precipitated, centrifuged, and redispersed in anhydrous toluene. The precipitation/redispersion treatment was conducted several times. **2) Synthesis of TOPO-Capped CdSe/CdS QTs:** CdSe/CdS tetrapods were generated by growing CdS arms on ZB-CdSe seeds. 0.207 g of CdO, 1.08 g of *n*-octadecylphosphonic acid (ODPA), 0.05 g of *n*-propylphosphonic acid (PPA), and 3.35 g of TOPO were degassed in a 25 ml three-neck flask at 120 °C for 1 h. The mixture turned into a clear solution when it was heated to 280 °C under N_2, after which the solution was cooled to 120 °C and degassed for 2 h. To synthesize the tetrapod, the reaction mixture was then heated to 300 °C. When temperature reached 300 °C, 1.5 g of TOP was

injected into the solution. Then 0.65 g of trioctylphosphine sulfide (TOPS) was injected into the solution, followed after 40 s by the injection of seeds (2 mg ZB-CdSe seeds) in 0.5 g of TOP. The reaction temperature was gradually increased to 315 °C (~1 °C/min) and maintained at that temperature for 20 min before cooling to room temperature. The yield of tetrapods was controlled using different amounts of PPA. The synthesized QTs were shown in Figure S13.

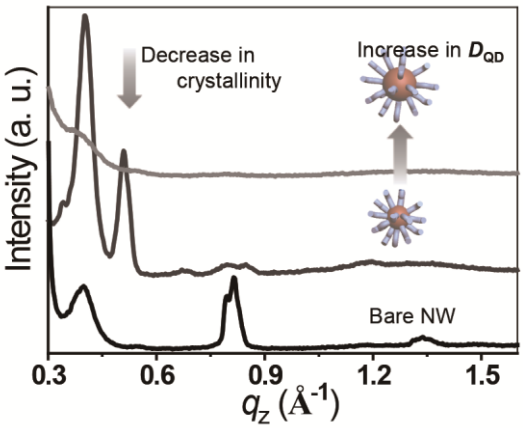

Figure S3. Out-of-plane line cut (q_z) profiles from GI-WAXS patterns as-cast thin film of P3HT-*b*-P2VP/QD solutions containing hybrid NWs as a function of QD size: (bottom) bare NWs, and after addition of (middle) ~4 nm QDs and (top) ~7 nm QDs, respectively. D_{QD} indicates a diameter of QD.

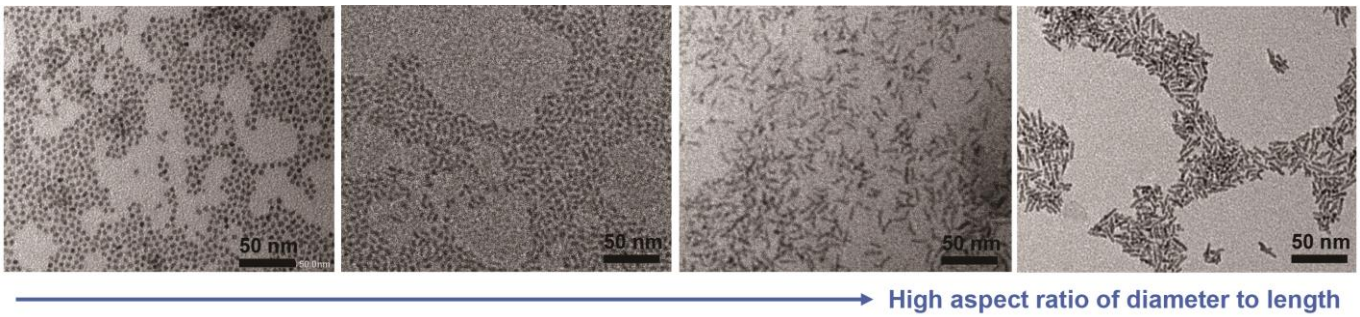

Figure S4. Synthesis of TOPO-capped CdSe QR with different aspect ratios of diameter to length. The seed diameter is ~4 nm.

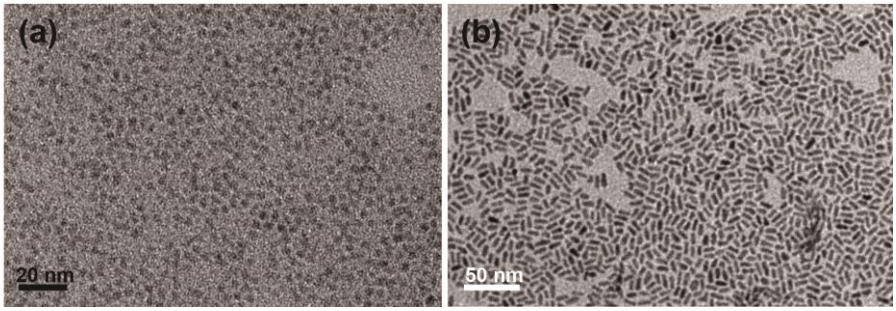

Figure S5. TEM images of TOPO-capped (a) CdSe QDs and (b) QRs used in this study.

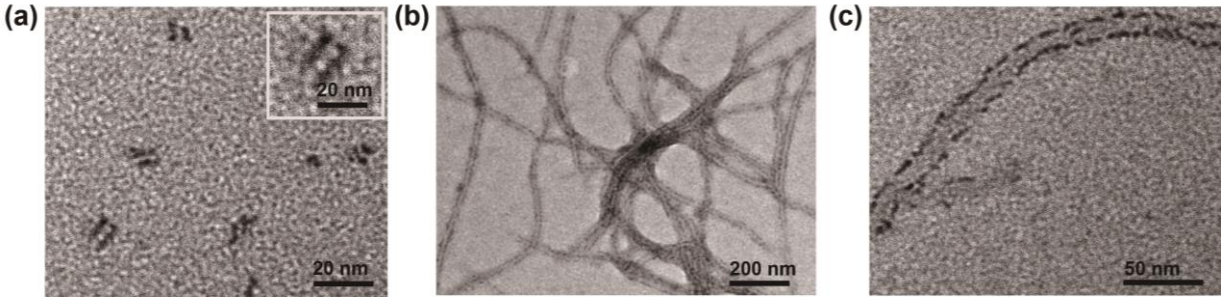

Figure S6. TEM images showing the structural evolution of P3HT-*b*-P2VP/QRs hybrid NWs formed by solution-biphase method: (a) dimeric crystal seeds (with a interparticle distance of ~9 nm) and (b) micrometer-long hybrid NWs. (c) Enlarged image of (b) representing the end-to-end QR array confined in a NW.

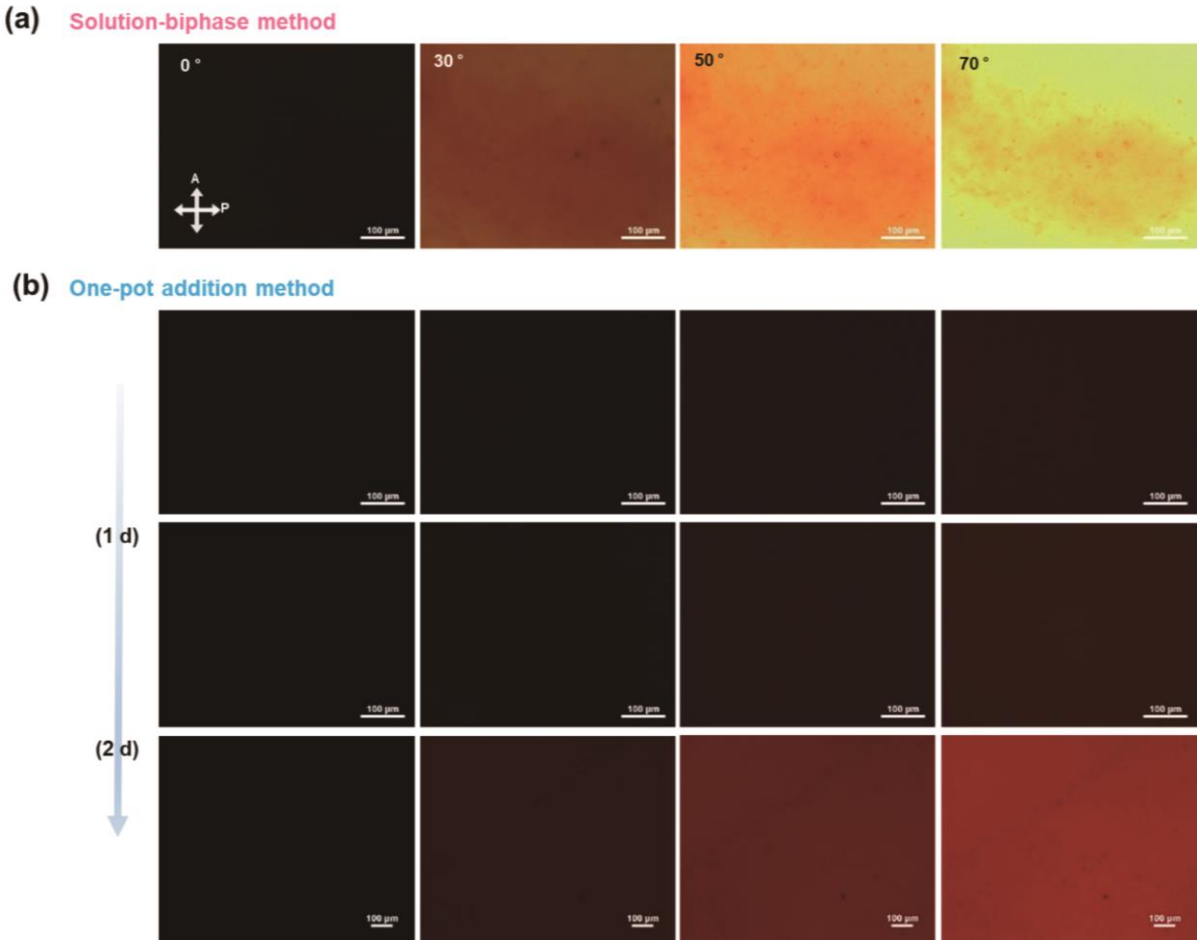

Figure S7. Polarized optical micrographs of P3HT-*b*-P2VP/QRs hybrid NW solutions prepared by (a) solution-biphase and (b) one-pot addition methods. The degree of rotation between crossed polarizer is labeled.

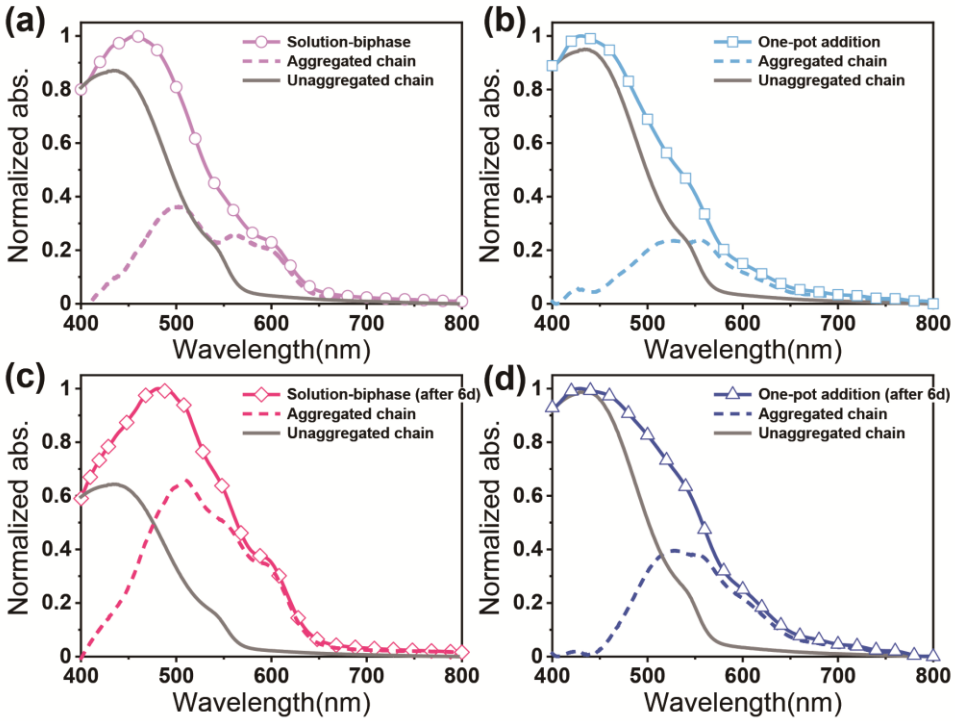

Figure S8. Experimental absorption spectra normalized to 0-2 absorption strength for P3HT-*b*-P2VP CP/CdSe QR formed by (a) solution-biphase method, (b) one-pot addition method, (c) solution-biphase method with aging for 6 d, and (d) one-pot addition method with aging for 6 d (in 2:1 chloroform/acetonitrile (v/v)). Each absorption spectrum was decomposed into a scaled CP/QR in chloroform (gray solid line), and aggregate spectrum (short dash line) modeled as a progression of Gaussian functions.

Table S2. Fraction of unaggregated and aggregated P3HT-*b*-P2VP chains for the formation of hybrid NWs (0.01 mg/mL of chloroform/acetonitrile), as calculated from absorption spectra depited in Figure S8

Methods	Unaggregated chains [%]	Aggregated chains [%]	$A_{0\text{-}0}/A_{0\text{-}1}$ [a]	W [b] [Free-exciton bandwidth, eV]
Solution-biphase	70.9	29.2	0.56	0.153
Solution-biphase after 6 d	50.6	49.4	0.58	0.144
One-pot addition	77.2	22.8	0.28	0.302
One-pot addition after 6 d	65.3	34.7	0.38	0.241

[a]Determined from the relative absorption intensity; [b]Determined by using Spano's model for weakly interacting H-aggregates.[S5]

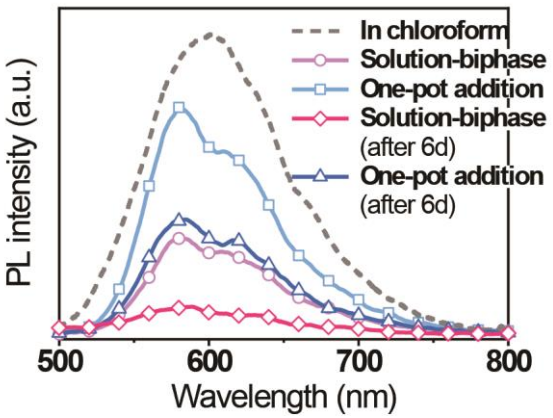

Figure S9. Photoluminescence spectra of P3HT-*b*-P2VP CP in 2:1 chloroform/acetonitrile (v/v) according to the different assembly methods (0.1 mg/mL).

3. Calculation of Location and Orientation of QR within the Hybrid NWs

By transmission electron microtomography (TEMT), the location and orientation of QRs within the NWs were identified through the calculating the tilted angles along to the longitudinal NW axis. We have assumed that there would be a long NW axis through the center of each QRs, so we were calculated the NW axis by ImageJ software according to the pixel points of x, y and z in each QR and indicated for a linear function. Center of QRs (C_{QRs}) was determined by an average value of pixel points of top and bottom (left and right) of QR.

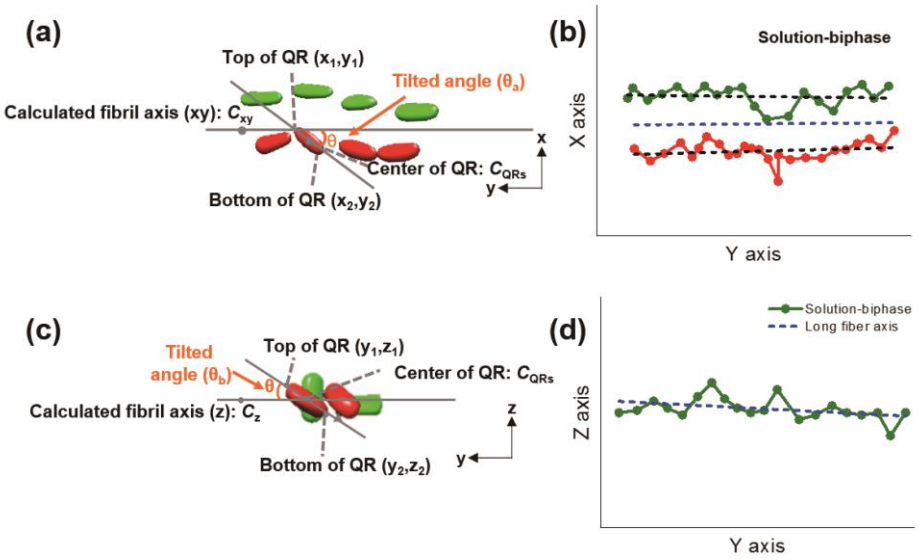

Figure S10. Calculation of offset angles of QRs within the hybrid P3HT-*b*-P2VP/QR NWs obtained from TEMT. Tilted angles of QRs within the hybrid NWs from (a,b) *xy* plane and (c,d) *yz* plane.

Table S3. Tilted angles (θ_a, θ_b) of QRs within the P3HT-*b*-P2VP/QRs hybrid NWs formed by solution-biphase method

Number of QRs	Z_top (px)	Z_bottom (px)	Z_center (px)	Y_left (px)	Y_right (px)	Y_center (px)	tilting angle(θ_a)	tilting angle(θ_b)
1	40.0	69.0	54.5	40.5	74.5	57.5	13.2	0.0
2	44.5	65.5	55.0	90.0	141.0	115.5	4.2	34.5
3	34.5	65.5	50.0	145.5	190.5	168.0	27.3	0.0
4	41.0	65.0	53.0	191.5	233.5	212.5	1.6	3.0
5	39.0	70.0	54.5	240.0	281.0	260.5	6.8	62.9
6	35.5	63.5	49.5	283.5	334.5	309.0	11.7	49.8
7	24.5	66.5	45.5	333.0	375.0	354.0	44.3	34.1
8	29.0	68.0	48.5	377.5	412.5	395.0	46.4	51.1
9	40.0	62.0	51.0	414.0	456.0	435.0	3.25	69.9

10	45.0	64.0	54.5	461.0	496.0	478.5	0.0	36.3
11	41.5	61.5	51.5	501.0	542.0	521.5	6.8	74.9
12	23.5	65.5	44.5	553.5	572.5	563.0	90.0	85.9
13	43.0	67.0	55.0	610.0	656.0	633.0	9.2	57.9
14	42.5	65.5	54.0	661.0	710.0	685.5	3.1	20.4
15	37.0	64.0	50.5	714.0	763.0	738.5	3.1	0.0
16	42.5	62.5	52.5	767.0	804.0	785.5	0.0	0.0
17	43.0	65.0	54.0	810.5	854.5	832.5	3.4	16.8
18	41.5	66.5	54.0	865.5	901.5	883.5	16.5	0.0
19	44.0	68.0	56.0	909.0	940.0	924.5	0.0	0.0
20	44.5	64.5	54.5	953.5	992.5	973.0	1.9	0.0
21	45.0	69.0	57.0	40.5	76.5	58.5	11.8	40.3
22	48.0	70.0	59.0	75.0	112.0	93.5	6.3	25.8
23	46.5	69.5	58.0	116.5	154.5	135.5	0.0	7.4
24	46.0	67.0	56.5	157.0	192.0	174.5	4.4	28.5
25	45.5	66.5	56.0	197.5	227.5	212.5	0.0	7.3
26	22.0	73.0	47.5	234.0	261.0	247.5	71.3	41.9
27	47.5	68.5	58.0	267.5	314.5	291.0	1.6	0.0
28	42.5	65.5	54.0	319.0	369.0	344.0	0.0	0.0
29	49.0	70.0	59.5	374.0	416.0	395.0	9.6	0.0
30	21.0	68.0	44.5	424.0	439.0	431.5	90.0	29.8
31	25.0	71.0	48.0	429.0	446.0	437.5	90.0	0.0
32	34.5	62.5	48.5	451.0	489.0	470.0	18.1	40.3
33	34.5	65.5	50.0	486.5	515.5	501.0	41.6	32.2
34	30.0	67.0	48.5	518.5	536.5	527.5	80.9	22.5
35	40.0	62.0	51.0	536.0	562.0	549.0	33.7	27.5
36	45.0	69.0	57.0	556.0	594.0	575.0	9.4	3.9
37	45.5	64.5	55.0	589.5	616.5	603.0	0.0	0.0
38	43.5	68.5	56.0	618.5	654.5	636.5	14.9	11.3
39	41.0	65.0	53.0	661.5	703.5	682.5	0.0	14.9
40	44.5	69.5	57.0	690.0	720.0	705.0	11.5	5.7
41	48.0	70.0	59.0	714.0	742.0	728.0	0.0	33.3
42	45.0	69.0	57.0	745.0	788.0	766.5	0.0	3.9
43	40.5	68.5	54.5	802.5	844.5	823.5	0.0	7.0
44	45.5	68.5	57.0	850.5	891.5	871.0	0.0	45.4
45	37.5	66.5	52.0	899.0	953.0	926.0	6.7	4.1

Table S4. Tilted angles (θ_b) of QRs within the P3HT-*b*-P2VP/QRs hybrid NWs formed by one-pot addition method

Number of QRs	Z_top (px)	Z_bottom (px)	Z_center (px)	Y_left (px)	Y_right (px)	Y_center (px)	tilting angle(θ_b)
1	65.5	146.5	106.0	27.5	48.5	38	79.8
2	54.5	156.5	105.5	256.5	280.5	268.5	-89.5
3	60.5	132.5	96.5	348	369	358.5	77.9
4	50.0	160.0	105.0	653.5	669.5	661.5	89.0
5	57.0	158.0	107.5	773.5	800.5	787	-88.8
6	59.0	155.0	107.0	1048	1067	1057.5	-65.8
7	85.5	162.5	124.0	1198.5	1214.5	1206.5	-87.1
8	41.0	131.0	86.0	47	70	58.5	88.7
9	39.5	155.5	97.5	141	167	154	-89.9
10	64.5	152.5	108.5	238.5	260.5	249.5	-87.4
11	55.0	148.0	101.5	435	460	447.5	-63.9
12	45.0	141.0	93.0	599.5	627.5	613.5	82.9
13	40.5	120.5	80.5	817	840	828.5	47.2
14	57.0	122.0	89.5	1046	1067	1056.5	59.3
15	35.0	135.0	85.0	1186	1205	1195.5	-86.6
16	46.0	134.0	90.0	52	66	59	86.1
17	88.5	144.5	116.5	237.5	249.5	243.5	-84.5
18	55.0	115.0	85.0	384	396	390	-86.7
19	79.5	130.5	105.0	496	503	499.5	83.9
20	52.0	100.0	76.0	614.5	624.5	619.5	82.9
21	81.5	122.5	102.0	671	686	678.5	87.3
22	70.0	125.0	97.5	738	757	747.5	85.8
23	97.0	146.0	121.5	56.5	71.5	64	-43.8
24	98.5	161.5	130.0	114	130	122	-82.7
25	82.0	132.0	107.0	359	372	365.5	-71.6
26	63.5	98.5	81.0	422.5	443.5	433	31.3
27	81.5	137.5	109.5	533	550	541.5	-71.6
28	63.0	112.0	87.5	574	586	580	-82.2
29	54.0	109.0	81.5	666	682	674	-88.0
30	79.5	115.5	97.5	727	742	734.5	-79.0
31	17.5	113.5	65.5	11	42	26.5	-84.9
32	39.0	125.0	82.0	97	127	112	-85.1
33	22.0	105.0	63.5	182.5	204.5	193.5	-87.5
34	32.5	116.5	74.5	305.5	326.5	316	-88.7
35	67.5	145.5	106.5	445	463	454	-84.1
36	51.0	131.0	91.0	17	35	26	85.6
37	35.5	101.5	68.5	152.5	180.5	166.5	-88.2

38	10.0	95.0	52.5	244.5	268.5	256.5	90
39	26.5	124.5	75.5	357	388	372.5	80.1
40	59.0	153.0	106.0	42	72	57	-73.4
41	61.0	151.0	106.0	120.5	138.5	129.5	83.7
42	68.0	143.0	105.5	175	200	187.5	-78.7
43	40.5	110.5	75.5	227	249	238	78.4
44	67.0	131.0	99.0	311.5	347.5	329.5	-70.3
45	21.0	103.0	62.0	382.5	418.5	400.5	-66.3
46	31.0	119.0	75.0	11	40	25.5	87.4
47	46.0	135.0	90.5	101	130	115.5	65.9
48	40.5	131.5	86.0	217	242	229.5	-83.5
49	61.0	136.0	98.5	321	350	335.5	-61.4
50	63.5	146.5	105.0	458.5	488.5	473.5	-72.4

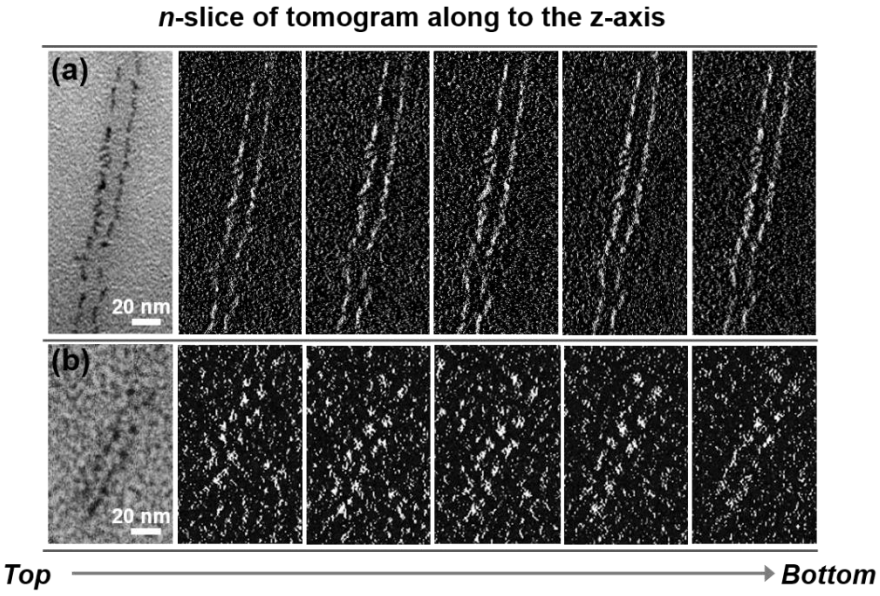

Figure S11. Galleries of selected computational xy-slices of the 3D tomographic volume of a tilt series of P3HT-*b*-P2VP/QRs nanohybrids formed by (a) solution-biphase and (b) one-pot addition methods.

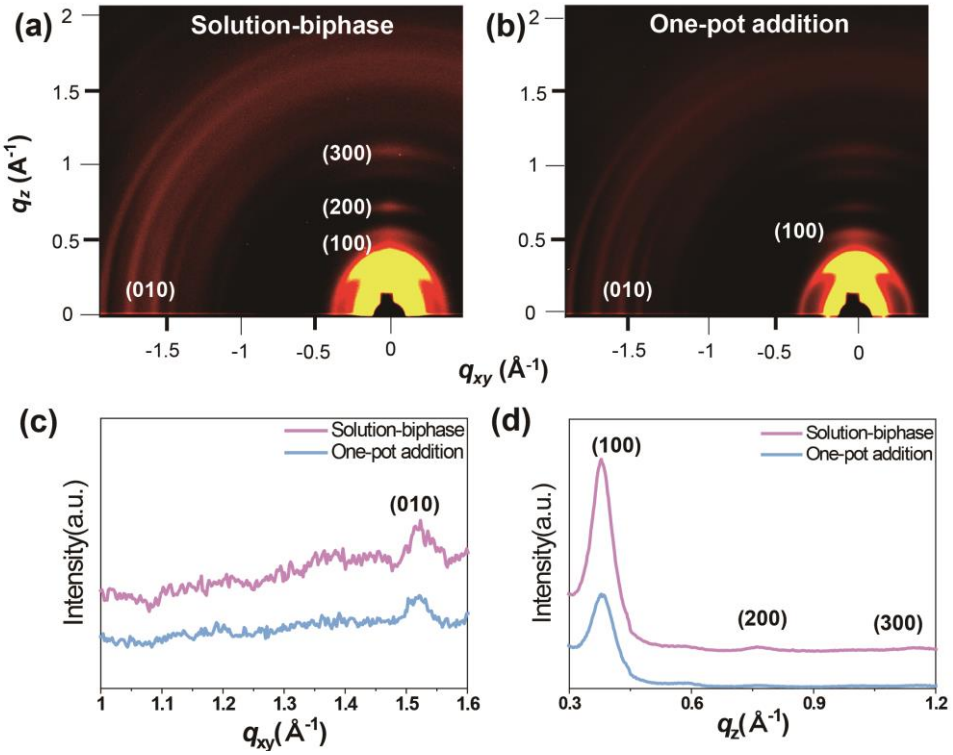

Figure S12. 2D GI-WAXS patterns of thin films as-cast from P3HT-*b*-P2VP/QRs solutions containing hybrid NWs formed by (a) solution-biphase and (b) one-pot addition methods. The in-plane q_{xy} and out-of-plane q_z directions are marked. (c,d) In-plane line cut (q_{xy}) and out-of-plane line cut (q_z) from (a) and (b), respectively.

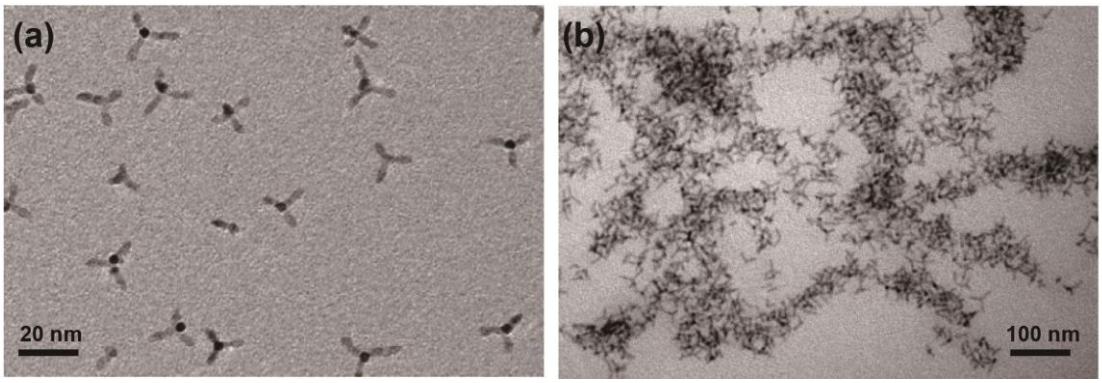

Figure S13. Synthesis of TOPO-capped (a) CdSe/CdS QTs (with seed diameter of ~3 nm and arm length of ~10 nm) and (b) coassembly with P3HT-*b*-P2VP CP in 2:1 chloroform/acetonitrile (v/v).

Supplementary Movies

We provide two movies as supplementary material: 3D visualization of hybrid NWs obtained from a tilting series of 2D TEM images. Surface rendering of reconstructed volume acquired from the TEMT. In order to distinguish the association mode (end-to-end or side-by-side coupling) of well-arranged QRs along the NWs, the QRs in a 1D alignment were marked in red and yellow.

Movie S1.avi｜ P3HT-*b*-P2VP/QRs hybrid NWs formed by solution-biphase method

Movie S2.avi｜ P3HT-*b*-P2VP/QRs hybrid NWs formed by one-pot addition method

4. References for Supporting Information

(S1) Kim, Y. J.; Cho, C. H.; Paek, K.; Jo, M.; Park, M.-k.; Lee, N. E.; Kim, Y.-j.; Kim, B. J.; Lee, E. Precise Control of Quantum Dot Location within the P3HT-*b*-P2VP/QD Nanowires Formed by Crystallization-Driven 1D Growth of Hybrid Dimeric Seeds. *J. Am. Chem. Soc.* **2014**, *136* (7), 2767–2774.

(S2) Wolcott, A.; Fitzmorris, R. C.; Muzaffery, O.; Zhang, J. Z. CdSe Quantum Rod Formation Aided By In Situ TOPO Oxidation. *Chem. Mater.* **2010**, *22* (9), 2814–2821.

(S3) Huang, J.; Kovalenko, M. V.; Talapin, D. V. Alkyl Chains of Surface Ligands Affect Polytypism of CdSe Nanocrystals and Play an Important Role in the Synthesis of Anisotropic Nanoheterostructures. *J. Am. Chem. Soc.* **2010**, *132* (45), 15866-15868.

(S4) Talapin, D. V.; Nelson, J. H.; Shevchenko, E. V.; Aloni, S.; Sadtler, B.; Alivisatos, A. P. Seeded Growth of Highly Luminescent CdSe/CdS Nanoheterostructures with Rod and Tetrapod Morphologies. *Nano Lett.* **2007**, *7* (10), 2951-2959.

(S5) Spano, F. C. Modeling Disorder in Polymer Aggregates: The Optical Spectroscopy of Regioregular Poly(3-Hexylthiophene) Thin Films. *J. Chem. Phys.* **2005**, *122* (23), 234701.